

Dual Modality: Mammogram and Ultrasound Feature Level Fusion for Characterization of Breast Mass

Minavathi, Murali .S, Dinesh M. S.

Abstract—detection of abnormalities in breast is done in different phases using different modalities and different biomedical techniques. These techniques and modalities are able to furnish morphological, metabolic and functional information of breast. Integrating these information assists in clinical decision making. But it is difficult to retrieve all these information from single modality. Multimodal techniques supply complementary information for improved therapy planning. This work concentrates on early detection of breast cancer which characterises the breast mass as malignant or benign by investigating the features retrieved from dual modalities: mammograms and Ultrasound. Architectural distortion (AD) with Spiculated mass is an important finding for the early detection of breast cancer. Such distortions can be classified as spiculation, retraction, and distortion which can be detected in mammograms. Spiculated masses carry a much higher risk of malignancy than calcifications or other types of masses. The proposed approach is based on the fusion of two modalities at feature extraction level with Z-Score Normalization technique to improve the performance of dual modality. Gabor filters are used to retrieve texture features from region of interest (ROI) of mammograms. Shape and structural features are retrieved from ROI's of Ultrasound. In addition to that some other discriminative features like denseness texture feature, standard deviation, entropy and homogeneity are also extracted from ROI's of both modalities. Feature level fusion is then achieved by using a simple concatenation rule. Finally classification is done using Support vector machine (SVM) classifiers to classify breast mass as malignant or benign. Receiver operating characteristic curves (ROC) are used to evaluate the performance. SVM classifiers achieved 95.6% sensitivity in characterising the breast masses using the features retrieved from two modalities.

Keywords— Mammogram, Ultrasound, Spiculated mass, Architectural distortion, Dual modality, SVM, Feature level fusion, Z-score Normalization.

I. INTRODUCTION

Multimodality information system provides complementary information to radiologists and has a great benefit for diagnosis and therapy. Radiologists in a normal follow-up face lot of difficulties in interpreting mammograms or ultrasonograms due to which more than half of breast

biopsies turn out to be negative. Thus it is desirable to have an alternative approach as a second line of defence. Towards that we have embarked on developing a dual modality model which fuses the features retrieved from mammogram and ultrasound. Any of the single modality used to analyse breast cancer is not rich enough to capture all classification information available in the image. Thus in normal medical diagnoses, images from different modalities are used to get a complete picture or information of abnormality. For example mammogram provides textural and morphological information where as ultrasound images give functional and metabolic information. Hence most of the limitations imposed by unimodal systems can be overcome by including multiple sources of information. Images from different modalities may be taken at different time, different resolutions and may be from different viewpoints so it is very difficult to simply overlay different images from different modalities to fuse the information. Integration of information in multimodality can occur at feature level or at decision level. Feature level methods combine several feature sets into a single fused one which is then used by any conventional classifier. Decision level fusion combines several classifiers resulting in strong final classifier. In this paper we focus on fusion at feature level which is believed to be a very promising method than others. Some of the important signs of breast cancer radiologists normally look for are: spiculated masses, micro calcifications, architectural distortions and bilateral asymmetry. Spiculated masses are characterized by radiating lines or spicules from a central mass of tissue. Spiculated masses carry a much higher risk of malignancy than calcifications or other types of masses [3]. Architectural distortion is the third most common finding of breast cancer. According to our survey 81% of spiculated mass and 48-60% of AD are malignant and 12-45% of cancers missed in screening are AD with spiculated masses. The detection sensitivity of the current methodologies for AD with Spiculated masses is low and there is a pressing need for improvements in their detection. Breast cancer does not always produce a visible mass, but it frequently disrupts the normal tissues in which it develops. This distortion of architecture may be the only visible evidence of the malignant process. The probability of malignancy increases as a lesion becomes more irregular in shape [4, 5]. Mammography and ultrasonography are currently the most sensitive noninvasive modalities for detecting breast cancer. A panel report issued from Institute of Medicine and National research council of National Academics stated that Mammography though useful wasn't always enough and health practitioners needed to investigate other complementary screening methods like ultrasound [6].

Manuscript published on 30 May 2013.

*Correspondence Author(s)

Minavathi, C S & E Department , Mysore University/ PET Research centre/ PESCE/ Mandya, Karnataka/ India.

Dr. Murali .S., C S & E Department, Mysore University/ MIT/ Mysore, Karnataka/ India.

Dr. Dinesh M.S., C S & E Department, Mysore University/ PET Research centre/ PESCE/ Mandya, Karnataka/ India.

© The Authors. Published by Blue Eyes Intelligence Engineering and Sciences Publication (BEIESP). This is an open access article under the CC-BY-NC-ND license <http://creativecommons.org/licenses/by-nc-nd/4.0/>.

It also says that mammography depicts about three to four cancers per 1000 women. But in women with dense breasts ultrasound depicts another three cancers per 1000 women. In addition, mammography produces a high false positive rate, and only about 525 of 1800 lesions that were sent to biopsy are malignant [6, 7]. Mammography has limitations in cancer detection in the dense breast tissue of young patients. Most cancers arise in dense tissue, so lesion detection for women in this higher risk category is particularly challenging. The breast tissue of younger women tends to be dense and full of milk glands, making cancer detection with mammography problematic. In mammograms, glandular tissues look dense and white, much like cancerous tumor. The reasons for the high miss rate and low specificity in mammography are, low conspicuity of mammographic lesions, noisy nature of the images, overlying and underlying structures that obscure features of the mammographic images [8]. The cancers found on ultrasound are almost all small invasive cancers that have not yet spread to the lymph nodes and therefore have good prognoses. Ultrasonography is proved to be more effective for women younger than 35 years of age and is an important adjunct to mammography [9]. Literature suggests that denser the breast parenchyma, higher will be the accuracy of malignant tumors in ultrasound images. However ultrasound itself has some limitations: low resolution, low contrast, blurry edges and speckle noise. So it is very difficult for a radiologist to read and interpret an ultrasound image. Though Mammography and ultrasonography are currently the most sensitive noninvasive modalities for detecting breast cancer, they have their own limitations. The above argument justifies that features retrieved from one modality are not sufficient to detect the abnormalities of breast cancer in early stages. Integration of multimodalities has been widely used for generating more diagnostic and clinical values in medical imaging [10]. Proper multimodality fusion techniques need to be employed. Thus our proposed work concentrates on designing image processing algorithms to extract features from dual modalities (ultrasound and mammogram) and to fuse them to improve the performance of characterization of breast masses. Multimodal techniques supply complementary information for improved therapy planning. As early detection of cancer is probably the major contributor to a reduction in mortality for certain cancers, images guided and targeted minimally invasive therapy has the promise to improve the outcome and reduce collateral effects.

II. REVIEW OF RELATED WORKS

In this section we give an insight of existing research works related to the proposed work. The topics related are classified under four sections. First we describe related works on pre-processing and segmentation for both mammogram and ultrasound, as we have finally fused the information retrieved from these two modalities. Second we focus on methods related to detection of abnormalities in breast ultrasound and mammogram. Third we describe the work carried out on different fusion techniques to fuse the features retrieved from different modalities. Finally we have highlighted the limitations of existing work which shows us the path to carry out the research by considering the limitations in the existing methods.

Pre-processing and segmentation on mammograms and ultrasound is carried out by several authors: Suckling *et al.* [23] segmented mammograms into four major components: background, pectoral muscle, fibro-glandular region and

adipose region, using multiple, linked self-organizing neural networks. Karssemeijer [24] used Hough transform detect the pectoral edge, is a popular technique. Ferrari *et al.* [25] segmented mammograms into skin-air boundary, fibro-glandular tissue, and pectoral muscle, based on the Hough transform. Georgsson [26] extracted the pectoral muscle by region growing. Fei Maa [27], introduced two image segmentation methods based on graph theory in conjunction with active contours to segment the pectoral muscle in screening mammograms. Mignotte and Meunier [28] used a statistical external energy in a discrete active contour for the segmentation of short axis images he says that this was well-suited in ultrasound images with significant noise and missing boundaries. The multi-scale optimization strategy of Heitz *et al.* [29] was adapted to perform the energy minimization.

Related works on detection of abnormalities in mammogram are: Tourassi [30] used fractal dimension to differentiate between normal and architectural distortion patterns in mammograms. An area under the receiver operating characteristics (ROC) curve of $Az = 0.89$ was obtained. Rangayyan and Ayres [31] applied Gabor filters to characterize oriented texture patterns and detect architectural distortion. FROC analysis shows the sensitivity of 0.79 at 8.4 false positives per image. Spiculation levels of breast mass boundaries are a primary sign of malignancy on mammography. Luan Jiang [32], developed an automated computerized method to detect spiculation levels. A quantitative spiculation index is computed to assess the degree of spiculation. The method achieved an overall classification accuracy of 66.4%, with 54.3% sensitivity and 78.3% specificity. Burhenne *et al.* [33] obtained a sensitivity of 75% of a commercial CAD system in the detection of architectural distortion. Evans *et al.* [34] reported that a commercial CAD system correctly identified 17 of 20 cases of architectural distortion. We focused on the detection of Spiculated Mass and AD for a number of reasons. Spiculated Mass carries a much higher risk of malignancy than calcifications or other types of masses. About 81% of Spiculated Mass and 48- 60% of AD is malignant [35]. Mudigonda *et al.* [36] presented a mass detection method that performs segmentation of objects based on intensity contours and texture flow-field analysis. Their study included 43 masses and 13 normal cases from the Mini-MIAS database with the performance of 81% and average of 2.2 FPs per image. Julia E. E. de Oliveira [37] proposed a method to classify spiculated mass and micro-calcification using Haar wavelet transform and SVM. An accuracy of 89.6% was achieved by them.

Survey on detection of abnormalities in breast ultrasound is: Cheng and Itoh [38] proposed a novel method for the automated detection of breast tumors in three dimensional ultrasonic images using fuzzy reasoning. 10 cases of malignant and 10 cases benign tumors are successfully extracted by the proposed method. Horsch [39] presented a method which involved thresholding a preprocessed image to enhance the mass structures. Madabhushi and Metaxas [40] worked by combining intensity, texture information, and empirical domain knowledge. Their method requires training but in the small database.

They showed that their method is independent of the number of training samples, shows good reproducibility with respect to parameters, and gives a true positive area of 74.7%. Yuji Ikedo and Daisuke [41] proposed a scheme for mass detection in whole breast ultrasound images using bilateral subtraction technique based on a comparison of the average gray values of a mass candidate region and a region with the same position and same size as the candidate region in the contra lateral breast. The sensitivity was 83% (5/6) with 13.8 (165/12) false positives per breast before applying the proposed reduction method. By applying the method, false positives were reduced to 4.5 (54/12) per breast without removing a true positive region. Dar and Chang [42] in their research used morphology operation, histogram equalization, and fractal analysis for classifying ultrasound images. The fractal analysis is applied to obtain the fractal texture features to classify the test cases of masses into benign and malignant. The accuracy rate was up to 88.80%. Yuji and Takako [43] proposed a computerized classification scheme to recognize breast parenchyma patterns in whole breast ultrasound (US) images. They employed Canonical discriminant analysis with stepwise feature selection for the classification of parenchymal patterns. The classification scheme resulted in the accuracy of 83.3% (10/12cases) in mottled pattern cases. An insight on works related to fusion is given here. Fabio Rolia et al. [11] have proposed a serial scheme on well-known benchmark face datasets and fingerprint dataset which combines two serially matchers at which the performance of the serial model is higher than parallel. Brunelli and Falavigna [12] have experimented using tanh method for normalization and weighted geometric average for fusion of voice and face biometrics. Hierarchical combination scheme is also used by them for a multimodal identification system. Kittler et al. [13] has used various fusion techniques on face and voice biometrics. He has experimented on sum, product, minimum, median, and maximum rules and have found that the sum rule outperformed others. He finally concluded that the sum rule is not significantly affected by the probability estimation errors and this explains its superiority. Hassan and A. S. Mohamed [14] presented a study of multimodal palm veins and signature identification by extracting the features of both modalities using morphological operations and Scale Invariant Features Transform (SIFT) algorithm. They have used simple sum rule to achieve feature level fusion for both modalities. They have applied discrete cosine transform (DCT) algorithm to reduce the feature vectors dimensionalities of feature extraction techniques. Finally they have stated that SIFT algorithm is more accurate and does not need more preprocessing steps to identify people. Han-ling and Fan [15] proposed a hybrid optimization algorithm to deal with multimodal (CT and MRI) medical images. They used mutual information as a similarity measure and proved that subvoxel accuracy can be achieved for an efficient image registration and can avoid getting into local optimum. Andrzej Krol and Ioana [16] have investigated an approach for co-registration of PET images with MR images in image fusion level. They proved that it is an alternative to surgical breast biopsy. Francis and Thomas [17] worked on fusion of data from mammography, ultrasound and non invasive infrared imaging modalities to improve early diagnosis. They concluded that data fusion will add early back into early detection of breast cancer.

From the literature it is clear that preprocessing algorithms identified the components of image belonging to the pectoral muscle but in most of the cases components found have ragged the edges and tend not to include the extreme edge of the pectoral muscle. The detection sensitivity of the current computer systems for Spiculated Mass and AD is low. Accurate and robust detection remains a technical challenge because the spiculated patterns are often subtle and varied in appearance. Due to lack of ground truth spiculation levels in the data set, assessing the performance of a method is also difficult. The works in medical image processing generally are not trying to perform fusion in feature level. But some of the work is been carried out in data level and image level fusion. In our proposed work we are introducing a new approach of fusing features of mammograms and ultrasound in order to improve the diagnosis by giving second opinion to the radiologist that hopefully reduce the rate of biopsy.

III. MATERIAL AND METHODS

In this paper we have used Ultrasound and mammogram images of same person which comprised of Architectural distortions with spiculated mass. For each image, a rectangular ROI including the AD with spiculated mass and the area around it were determined by an experienced radiologist. The radiologist also depicted mass contours and has classified them as regular or irregular.

Mammography whether film or digital is a best choice of screening for women who are less than age 40. But for younger women and dense breast women it is not an adequate choice. Though Ultrasound is a commonly used diagnostic tool, it is not FDA approved for screening.

Fusion of information can be done in feature level, data level or decision level. Feature level methods combine various features into single fused one which can be later used by conventional classifier. On the other hand decision level fusion combines several classifiers to make a stronger classifier which is also called as post classification fusion.

The purpose of our work is to demonstrate the fusion of features from mammogram and breast ultrasound that is not way off in future, but one that can be utilized today. Multimodality is not a new concept but the inclusion of feature level fusion to mammogram and ultrasound modalities to detect AD with spiculated mass is rare. Our objective is to show how feature level fusion in multimodality helps in detecting breast cancer.

The proposed dual modality system combines the structural and functional behavioural trait of mammogram and ultrasound modalities as shown in Fig.1. We have extracted texture features and directional features from mammograms using Gabor filters, gradient orientation and phase portraits. Using angle of curvature method and intensity based method functional features like acoustic shadow and shape features are retrieved from ultrasound. As Mammogram and Ultrasound are independent modalities, we need to normalize the features. Feature Normalization is done using Z-score, Min-Max and Tanh (TH) methods for feature level fusion. Support vector machine (SVM) classifiers are used to classify the fused features.

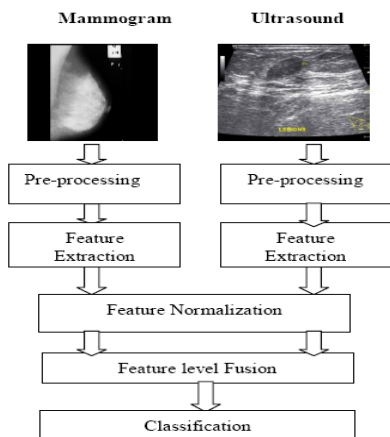


Fig.1 Proposed Dual modality system

A.Characterisation of mass using single modality mammogram

Biomedical images are often affected and corrupted by various types of noise and artifacts. To remove noise like artifacts and pectoral muscle region without causing any distortion or loss of the desired information in the image of interest we have used connected component algorithm and anisotropic diffusion algorithm. Anisotropic diffusion is an important segmentation method which creates a piecewise constant image so that the segmentation boundaries can be easily obtained. Nonlinear partial differential equation used for smoothing image on a continuous domain:

$$\frac{\partial I}{\partial t} = \text{div}[c(\|\nabla I\|) - \nabla I] \rightarrow (1)$$

$$I(t=0)=I_0$$

Where ∇ is the gradient operator, div the divergence operator $\|\nabla I\|$ denotes the magnitude, $c(x)$ the diffusion coefficient, and I_0 the initial image. Proposed diffusion model not only provides different degrees of smoothing for intra-regions but also actively provides different degrees of sharpening for edges in inter-regions. The results of pre-processing are shown in the Fig 2.

To extract features from mammograms we have developed a new computerised method to detect spiculated masses with Architectural Distortions. The method is based on the distribution of the mammary gland which is approximated to linear structures. Overall method of detecting AD with spiculated mass using a single modality mammogram is shown in Fig 3. In normal breast, the direction of the distribution tends toward the nipple and in an abnormal breast, it tends toward suspect areas [5]. Based on the linear structure of mammary gland, we evaluate local structure of mammary ducts. We then focus on characterizing the degree of concentration of mammary ducts to a specific point. Additional features like denseness texture feature, standard deviation, entropy and homogeneity are also considered.

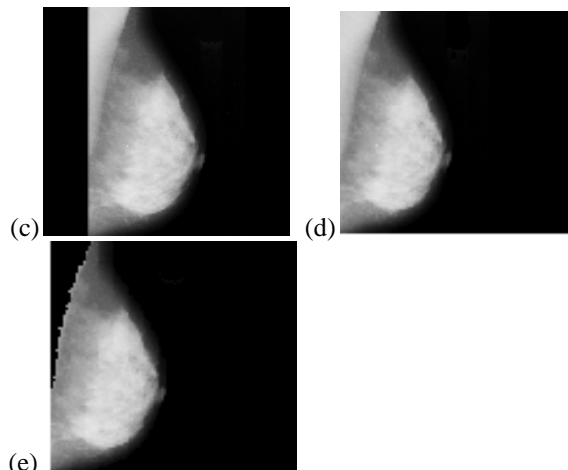
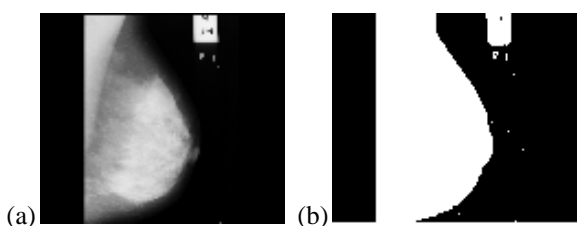


Fig. 2 (a) Original image Mdb004 in MiniMIAS atabase, (b) Binary image showing different components of image, (c) Artifacts removed image, (d) Normalized image, (e)Pectoral muscle identified and removed.

In the present work we have used Gabor filters as line detectors. In order to extract the texture orientation at each pixel of a mammogram, we filter the mammogram with a bank of Gabor filters of different orientations [5, 18]. The Gabor filter kernel oriented at the angle $\theta = -\pi/2$ is given by:

$$g(x, y) = \frac{1}{2\pi\sigma_x\sigma_y} \exp\left[-\frac{1}{2}\left(\frac{x^2}{\sigma_x^2} + \frac{y^2}{\sigma_y^2}\right)\right] \rightarrow (2)$$

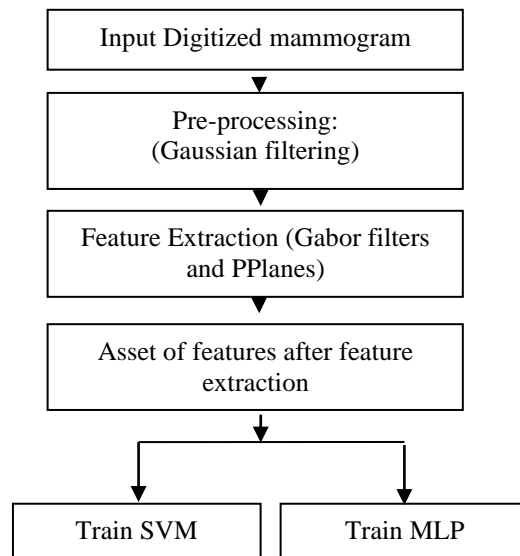


Fig. 3 Block diagram showing Detection of AD with spiculated mass in mammogram

Kernels at other angles can be obtained by rotating this kernel. We have used 180 kernels with angles spaced evenly over the range $[-\pi/2, \pi/2]$. A Gabor filter can provide good detection accuracy for linear patterns with thickness up to 0.8 mm [5, 18]. It is desirable to reduce the influence of the low-frequency components of the mammographic image in the orientation field magnitude, since the low-frequency components are not related to the presence of oriented structures in the image.

Therefore, the mammographic image is high pass filtered prior to the extraction of the orientation field. Gaussian filters are used for low pass filtering. In order to extract orientation at each pixel of magnitude image obtained after Gabor filtering, gradient based orientation extraction is used. Here gradient vectors are calculated by taking partial derivatives of image intensity at each pixel in Cartesian coordinates.

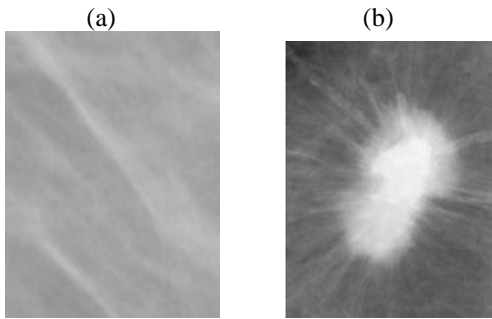


Fig. 4 (a) Image of Normal breast structure, (b) Image of AD with Spiculated mass breast structure

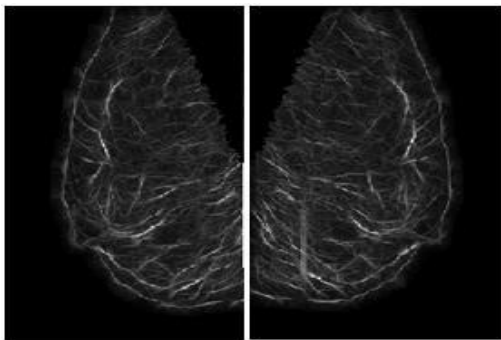


Fig.5 Magnitude image mdb117 and mdb118 after Gabor filtering

AD with Spiculated masses have stellate appearance as shown in Fig 4(b). The size of the lesion ranges from few millimeters to centimeters.

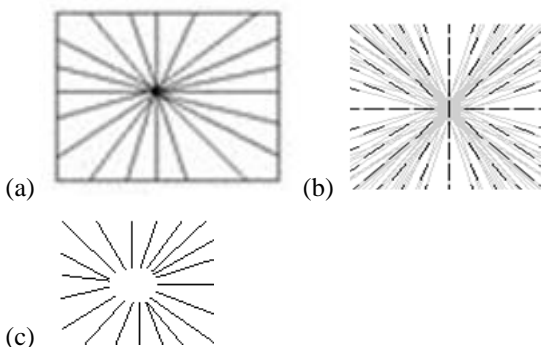


Fig. 6 (a) Synthetic node drawn using PPlanes, (b) Orientations drawn, (c) stellate appearance of AD with spiculated mass

Our process for detecting AD with Spiculated masses is further performed by searching for node or star like stellate structures in the image. Phase Planes provide an analytical tool to study systems of first-order differential equations. We have drawn node and star maps using phase planes (PPlanes) and it is compared with the gradient orientation image. As we need some measure of distance between two orientation

fields we have applied flow field analysis using distance measure (nonlinear least squares) [5,21] and the degree of distortion is calculated. The measure that we use is the area of the triangle formed by the oriented segments, which is

$$A_{i,j} = \frac{1}{2} R_1 R_2 \left| \sin(\theta_{1,i,j} - \theta_{2,i,j}) \right| \rightarrow (3)$$

O1 and O2 are two discrete orientation fields where O1 is the orientation extracted from the map drawn from PPlanes and O2 is the gradient orientation of mammographic image. Length of orientation line segment is represented by $R_{k,i,j}$ in orientation field O_k at location (i, j). Angle subtended by this line segment is represented by θ_k . When two segments have the same orientation the area becomes zero. The sum of these differences over the entire field is represented by S and is given by:

$$S = \sum_{i,j \in W} A_{i,j} \rightarrow (4)$$

The presence of stellate appearance (strong node or star point indicates the sites of AD with spiculated mass.

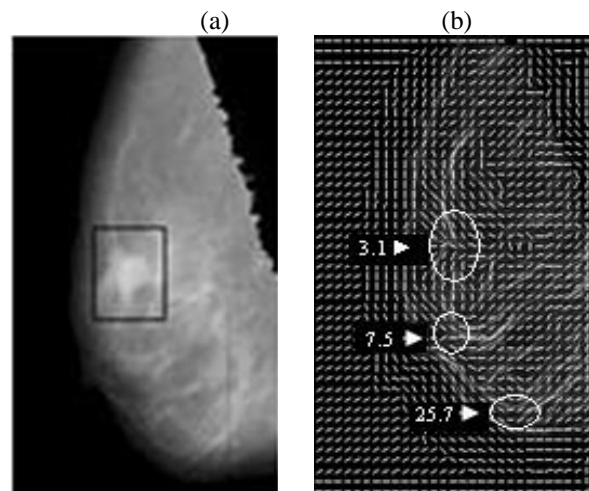


Fig. 7 (a) Ground truth, (b) Detected node points showing S values.

The features that constitute image texture extracted above are not sufficient for classification, thus some other characteristic features that are concerned with spatial organization of gray level primitives are considered. Additional features that we have extracted from gradient orientation image are denseness texture feature, standard deviation, entropy and homogeneity. Where denseness texture feature D is defined as:

$$D = \sum_{\forall(r,c) \in E_h} E(r,c) + \sum_{\forall(r,c) \in E_v} E(r,c) \rightarrow (5)$$

Where E is morphologically eroded image. E_h and E_v indicate the eroded images by a horizontal and a vertical structuring element, respectively. Denseness feature value D close to zero indicates that the area has a few locally dense regions, while a value far off zero indicates it has many locally dense regions.

Table 1. Analysis done on 61 suspected regions

	Disease	
Test	Present	Absent
Positive	22 (TP)	10 (FP)
Negative	4 (FN)	25 (TN)

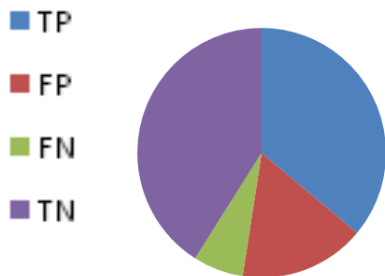


Fig. 8 Pi chart showing the analysis done on 61 suspected regions

Support vector machine (SVM) classifier is used to classify AD with spiculated mass and Normal breast tissue. The reason why SVM is selected for classification in our work is [20]:

- SVM has good capacity of generalization.
- SVM is highly robust and work well with images.
- The theory of SVM is well defined and has a very good base of mathematics and statistics.
- Over training problem is less compared to other neural network classifiers.

Kernel function $k(x, y)$ in SVM plays very important role in mapping input vector to high dimensional feature space. By using different kernel functions like Gaussian Radial Basis Function (RBF), Polynomial, Linear, quadratic, etc., SVM implements a variety of learning machines. In our work we have used the following kernel functions:

- Gaussian RBF kernel:

$$k(x, y) = \exp \left[-\frac{\|x-y\|^2}{\sigma} \right] \rightarrow (6)$$

- Polynomial kernel:

$$k(x, y) = ((x \cdot y) + \text{coeff})^p \rightarrow (7)$$

- Linear kernel :

$$k(x, y) = (x \cdot y) \rightarrow (8)$$

The process of classification has two phases: training phase and testing phase. In training phase data set which is labeled as Normal or AD with Spiculated mass are given to classifier and the classifier is trained. In testing phase, unknown dataset are given to the classifier for actual classification. Data set was created by collecting and getting the ground truth marked images from expert radiologists trained with those kinds of images. Dataset was divided as Training set 70% and Testing set 30%. For cross validation we used leave-one-out scheme. The performance of SVM classifier is given in table 1. The performance of the classifier is assessed in terms of sensitivity and specificity. Where sensitivity is the proportion of actual positives which are correctly identified and specificity is the proportion of negatives which are correctly

classified. The sensitivity achieved by SVM classifier is 93.52%.

Table 2. Results of SVM classifier

Kernel Function	Sensitivity (%)	Specificity (%)
Gaussian RBF	94.78	89.67
Polynomial	85.14	72.39
Linear	84.82	80.15

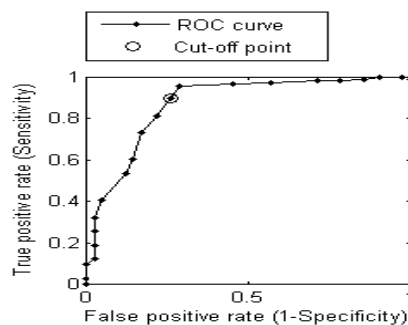


Fig. 9 ROC curve depicting the performance of SVM classifier Gaussian RBF kernel.

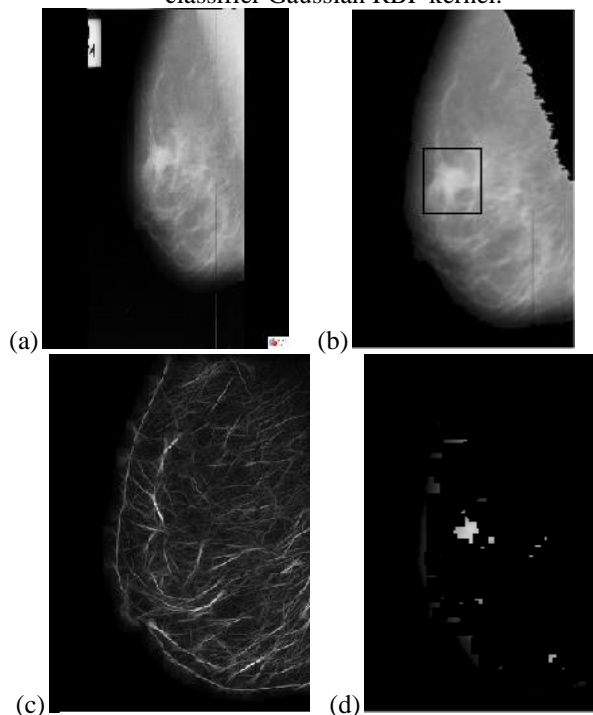


Fig. 10 (a) Original mammogram , (b) Pre-processed image showing the position of AD, (c) line strength image after applying Gabor filter, (d) Probability image

B. Characterisation of mass using single modality Ultrasound

Ultrasound (US) is an important adjunct to mammography in breast cancer detection as it doubles the rate of detection in dense breasts and also does dynamic analysis of moving structures in breast.

Architectural distortions and spiculated masses with Architectural distortions on mammography are considered to be one of the most indicators of breast cancer. But recently AD and AD with spiculated mass has been detected via ultrasonography also. Distortion refers to presence of radiating structure concentrated at a point as shown in Fig. 11.



Fig. 11 Appearance of AD in Ultrasound

As the spatial resolution of ultrasound is not good detection of AD even in the absence of definite mass is difficult. Thus we are concentrating on detection of AD with spiculated mass in our work. Block diagram in Fig

12 shows the complete process of detecting AD with spiculated mass using a single modality ultrasound. Ultrasound images are first pre-processed using Gaussian smoothing to remove additive noise and anisotropic diffusion filters to remove multiplicative noise (speckle noise). For segmentation active contour method is used to extract a closed contour of filtered image which is the boundary of the spiculated mass. During feature extraction spiculations which make breast mass unstructured or irregular are marked by measuring the angle of curvature of each pixel at the boundary of mass. To classify the breast mass we have used the structure of mass in accordance with spiculations and elliptical shape.

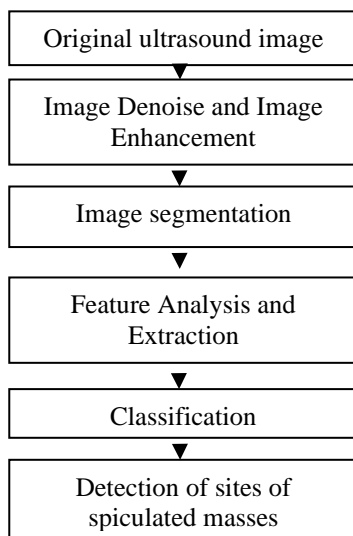


Fig. 12 Block diagram showing Detection of AD with spiculated mass in ultrasound

Several features might be able for classification. Too many irrelevant features not only derived from an image. But more features make the classifier complicated, but also will reduce the accuracy of the classification. The most important issue is to select features that are able to represent the characteristics of spiculated masses in the breast ultrasound images. Spiculations are the small needle like structures found in

malignant mass which shows uncontrollable multiplication of breast cells. These spiculations will make the breast masses unstructured and irregular [6].

The first feature retrieved is the spiculation feature of mass by finding and roughly ellipse. Thus as a second feature we consider shape of the mass by fitting the contour to ellipse. Based on these features the spiculated malignant mass can be significantly discriminated from the benign masses by the classifier. In breast ultrasound images, spiculations and angular margins are the significant characteristics. Spiculations produce the higher positive predictive value of malignancy. Also, the hyperechogenicity, well-circumscribed lobulation, ellipsoid shape and a thin capsule are the significant characteristics of benign masses in breast ultrasound images [6, 19].

The angle of curvature of every pixel at that boundary of the mass is considered. At every pixel the angle of curvature is found by projecting lines from that pixel to some appropriate pixels and the angle between the lines are found and is as shown in Fig 13. Spiculated regions will be having lesser angle of curvature and thus the measured angle of curvature at each pixel is compared with certain range of angle, showing the spiculated region. Here we have considered spiculated angle range as 45° to 60° and if any pixels showing this feature are found, they are marked for analysis as shown in Fig. 14(d).

$$\text{where } \phi = \tan^{-1} \left[\frac{m_2 - m_1}{1 + m_1 * m_2} \right] \rightarrow (9)$$

$$\text{and } m_1 = \frac{(b-y)}{(a-x)}, \quad m_2 = \frac{(d-y)}{(c-x)} \rightarrow (10)$$

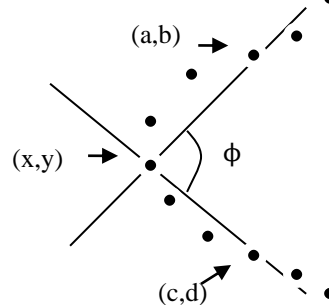


Fig. 13 Angle of curvature at pixel (x,y) found by projecting lines from that pixel

Shape of the mass is also one of the important features that can be considered for classification of mass as benign or malignant in ultrasound images. The proportion of width and height of the mass and its ellipsoid shape are some of the important features which help us to decide the mass as benign or malignant [22]. A mass with ellipsoidal shape shown in Fig. 15(a) will increase the probability of mass being benign. Most of the malignant masses will normally produce projections from the surface of the mass which extend towards nipple, thus they will be taller than wider as shown in Fig. 15(b).

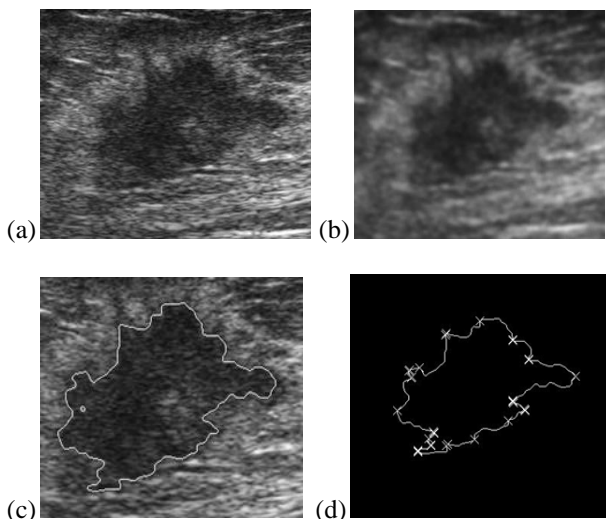


Fig. 14 (a) Ultrasound image showing Spiculated mass, (b) Image after preprocessing, (c) Image after segmentation, (d) Mass boundary on which spiculations are marked with “x”.

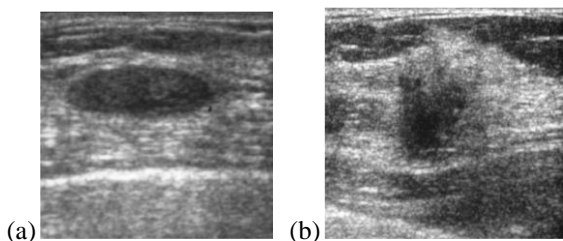


Fig. 15 (a) Mass with elliptical shape (benign), (b) Mass which is taller than wider (malignant)

To fit an ellipse to the contour of mass, we first consider the contour of mass which is already retrieved in previous section. Let $(c1,c1)$ be the centroid of mass contour and the maximum path passing the point $(c1,c1)$ be the major axis ‘a’ and the minimum path through $(c1,c1)$ is considered as a minor axis ‘b’. Angle between X-axis and major axis is considered to be ‘ θ ’. Mathematically an ellipse may be specified as:

$$x(t) = c1 + a \cos t \cos \theta - b \sin t \sin \theta \rightarrow (11)$$

$$y(t) = c2 + b \sin t \cos \theta + a \cos t \sin \theta \rightarrow (12)$$

Where t is interval angle $(0 < t < 2\pi)$

The standard deviation of the shortest distance is the best fit of mass contour by an ellipse. Shortest distance can be defined as

$$S(i) = |E_i H_i| \quad i=1,2,3,\dots,N \rightarrow (13)$$

Where N is number of pixels on mass contour. Standard deviation of shortest distance is given by

$$SD = \sqrt{\frac{1}{N-1} \sum_{i=1}^N [S(i) - \frac{1}{N} \sum_{i=1}^N S(i)]^2} \rightarrow (14)$$

A mass is said to produce acoustic shadow if the ultrasound is attenuated when crossing through it. If a mass generates acoustic shadow it is considered as malignant. Appearance of mass with acoustic shadow and without acoustic shadow is shown in Fig. 17 (b).

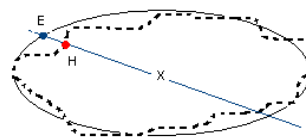


Fig. 16 shows the shortest distance in the best fit ellipse. Point ‘X’ in the centre is centroid of mass contour

Acoustic shadow can be determined by considering intensity as a main factor. To find whether mass has generated shadow or not, we first calculated the mean intensity of the region under the mass and compare it with the mean intensity of the region at the same level which is not covered by the mass. We have used SVM for classification. Using support vectors SVM finds adequate hyper plane to separate the groups. After separation, cases belonging to one category remains in one side of the plane and other cases will remain on the other side of the plane [6, 20].

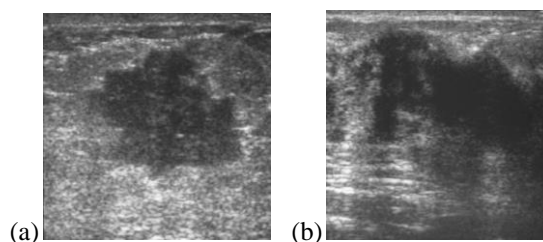


Fig. 17 (a) Mass without Acoustic shadow, (b) Mass with acoustic shadow.

The features we have considered are discriminative and effective in characterizing the mass in ultrasound images. Using a single feature as parameter to discriminate is always a tradeoff between the sensitivity and specificity. The tradeoff is due to that each feature parameter is mainly related to its nature. So we have considered the features like spiculated feature, acoustic shadowing, elliptical shape feature, entropy and standard deviation for discrimination. The data set for ultrasound is also created by collecting and getting the ground truth marked images from expert radiologists trained with those kinds of images. Dataset was divided as Training set 70% and Testing set 30%. For cross validation we used leave-one-out scheme. The performance of SVM classifier is given in table 3. The performance of the classifier is assessed in terms of sensitivity and specificity. Where sensitivity is the proportion of actual positives which are correctly identified and specificity is the proportion of negatives which are correctly classified. The sensitivity achieved by SVM classifier is 92.7%.

Feature level fusion

The features retrieved from mammogram are structural features and that from ultrasound are functional features and they are dissimilar in terms of dimension. For fusion of features we needed coherent dataset from both modalities which belong to a same person. Data set was created by collecting and getting the ground truth marked images from expert radiologists trained with those kinds of images. All images in our dataset contained only one abnormality (AD with spiculated mass).



As discussed in previous sections both modalities will output a collection of features. The fusion process fuses this collection of features into a single feature set.

Table 3. Results of SVM classifier for Ultrasound

Kernel Function	Sensitivity (%)	Specificity (%)
Gaussian RBF	92.7	90.3
Polynomial	89.4	90.1
Linear	88.5	89

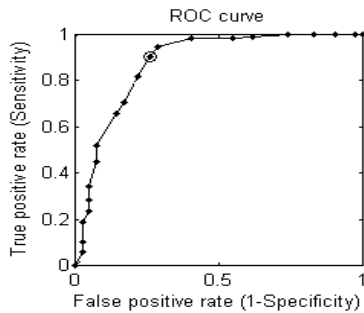


Fig. 18 ROC Curve depicting the performance of SVM classifier with sensitivity of 92.7% and AUC=0.88.

Feature level fusion is a medium level fusion strategy which performs well, if the features are homogenous. If the features are heterogeneous, then it requires normalization to convert them into a range that makes them more similar. We have used three well-known normalization methods:

- Min-Max (MM)
- Z-score (ZS)
- Tanh (TH)

Min-Max (MM): Min-Max is a method which maps the raw scores (s) to the [0, 1] range and it is given by:

$$n = \frac{s_i - \min(s)}{\max(s) - \min(s)} \rightarrow (15)$$

Where the quantities max(s) and min(s) specify the end points of the score range.

Z-score (ZS): ZS method helps in transforming the scores to a distribution with mean of 0 and standard deviation of 1.

$$n = \frac{s_i - \text{mean}(s)}{\text{std}(s)} \rightarrow (16)$$

Where the operators mean() and std() denote the arithmetic mean and standard deviation operators, respectively.

Tanh (TH): TH method is a robust statistical technique. It maps the raw scores to the (0, 1) range which is given by:

$$n = \frac{1}{2} \left[\tanh \left(0.01 \frac{(s_i - \text{mean}(s))}{\text{std}(s)} \right) + 1 \right] \rightarrow (17)$$

IV. EXPERIMENTAL RESULTS AND DISCUSSION

The feature level fusion is realized to be simply concatenating the feature points obtained from different sources of information. The concatenated feature vector has better discrimination power than the individual feature vectors. The main aim of this fusion is to test if the fusion of two sets of features can improve classification accuracy. A fair assessment should be based on the feature vectors with the same dimensionality. In this feature level fusion, proper

normalization is required to address the difference in measurement scale because during fusion we augment features that are retrieved from different extraction methods. One major problem associated with this fusion scheme is that the same classifier has to be applied to the fused feature set. But the feature sets from both the modalities mammogram and ultrasound may have different utilities and may have their own individuality favored classifiers. Because it is known that classification performance depends mainly on the characteristics of the data. It is difficult to find a single classifier that works best on all given data sets.

Support vector machines (SVM) are a learning tool based on modern statistical learning method that classifies binary classes. SVM has been shown to perform better than many other classification algorithms due to several reasons [5, 20]:

- SVM has good capacity of generalization.
- SVM is highly robust and work well with images.
- The theory of SVM is well defined and has a very good base of mathematics and statistics.
- Over training problem is less compared to other neural network classifiers.

Thus we have used SVM classifiers to classify the fused feature vector. Implementation is done using MATLAB. For experimentation we have randomly partitioned the dataset training and testing data with the proportion of 70% and 30% respectively. We have used receiver operating characteristic curve (ROC) to evaluate the performance. ROC graphically represents the true positive rate as a function of false positives rate.

Table 4. Performance of SVM classifier for dual modality using Min-Max normalization

Kernel Function	Sensitivity (%)	Specificity (%)
Gaussian RBF	80.1	71.7
Polynomial	72.3	60.9
Linear	78.5	75.0

Table 5. Performance of SVM classifier for dual modality using Z-Score normalization

Modalities	Sensitivity (%)	Specificity (%)
Mammogram	93.52	89.67
Ultrasound	92.7	90.3
Dual modality	95.6	90.15

Table 6. Performance of SVM classifier for dual modality using Tanh normalization

Kernel Function	Sensitivity (%)	Specificity (%)
Gaussian RBF	85.2	81.3
Polynomial	88.7	76.2
Linear	77.2	73.6

Table 7. Comparison of Results

Kernel Function	Sensitivity (%)	Specificity (%)
Gaussian RBF	95.6	91.1
Polynomial	90.7	88.9
Linear	91.3	86.2

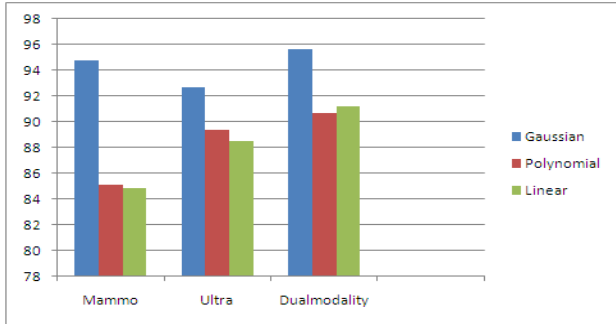


Fig. 19 Comparison of performance of all three proposed methods using SVM classifier.

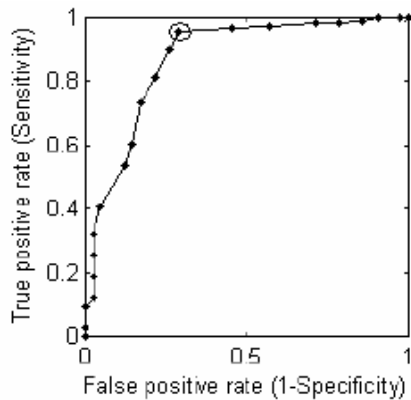


Fig. 20 ROC Curve depicting the performance of SVM Classifier for Dual modality with sensitivity 95.6%

V. CONCLUSION AND FUTURE WORK

In this study information from multiple modalities such as mammogram and ultrasound was used to classify the breast mass as benign or malignant. The features retrieved from mammogram are spiculation feature and denseness texture feature and that from ultrasound are spiculation feature, shape feature and shadowing feature. From both modalities we have retrieved some additional features like: standard deviation, entropy and homogeneity. Both modalities supply complementary information which is helpful in discriminating benign from malignant mass. The results for the fusion model were compared with individual modalities to understand the effects of more than one modality. Results show that the multimodal fusion improved the performance to classify breast mass more accurately. Accuracy can still be improved if standard dataset is made available for fusion. Comparative study in ultrasound methods can be made more accurate if standard dataset is available. Research towards multimodality in breast cancer analysis is very less. We can work in different directions of multimodality to improve the sensitivity rate in detecting breast cancer as early as possible.

REFERENCES

1. M. A. Wirth, Nonrigid Approach to Medical Image Registration: Matching Images of the Breast , Ph.D. Thesis, RMIT University, Melbourne, Australia, 2000.
2. R. Gupta and P. E. Undrill, The use of texture analysis to delineate suspicious masses in mammography, Phys. Med. Biol., vol. 40, pp. 835–855, 1995 .
3. Mehul P. Sampat, Gary J. Whitman, Alan C. Bovik, and Mia K. Markey, “ Comparison of Algorithms to Enhance Spicules of Spiculated Masses on Mammography”, Journal of Digital Imaging, Vol 0, No 0 (Month), 2007: pp 1-8.
4. Kopans,” Breast Imaging”, New York: Lippincott-Raven Publishers, 1998.
5. Minavathi, Murali. S and M.S.Dinesh, Model based approach for Detection of Architectural Distortions and Spiculated Masses in Mammograms, International Journal on Computer Science and Engineering (IJCSE) ISSN : 0975-3397 Vol. 3 No. 11 November 2011 page no: 3534.
6. Minavathi, Murali. S and M.S.Dinesh, curvature and shape analysis for the detection of spiculated masses in breast ultrasound images, IJMI International Journal of Machine Intelligence ISSN: 0975–2927 & E-ISSN: 0975–9166, Volume 3, Issue 4, 2011, pp-333-339.
7. M. A. Wirth, Nonrigid Approach to Medical Image Registration: Matching Images of the Breast, Ph.D. Thesis, RMIT University, Melbourne, Australia, 2000.
8. Marnell Jameson, Ultrasound as a breast cancer test is becoming more accepted, Los Angeles Times , 000037057 June 14 , 2004.
9. E.A Sickles, R.A. Filly, P.W. Callen, Breast detection with sonography and mammography, AJR, 140:843-845, 1983.
10. H. Gholam Hosseini, A. Alizad and M. Fatemi, Integration of Vibro-Acoustography Imaging Modality with the Traditional Mammography, Hindawi Publishing Corporation International Journal of Biomedical Imaging Volume 2007, Article ID 40980, 8 pages doi:10.1155/2007/40980.
11. Gian Luca Marcialis, Fabio Roli, Luca Didaci(2009) Pattern Recognition 42(11): 2807- 2817.
12. R. Brunelli, D. Falavigna, "Person identification using multiple cues," IEEE Transactions on Pattern Analysis and Machine Intelligence 1995.
13. J. KITTLER, R. P.W. DUIN, "The combining classifier: to train or not to train," in Proceedings of the International Conference on Pattern Recognition, vol. 16, no. 2, pp. 765–770, 2002.
14. Hassan Solimanv, Abdelnasser Saber Mohamed, Ahmed Atwan, Feature Level Fusion of Palm Veins and Signature Biometrics , International Journal of Video & Image Processing and Network Security IJVPNS-IJENS Vol: 12 No: 01 28.
15. Han-ling ZHANG , Fan YANG, Multimodality Medical Image Registration Using Hybrid Optimization Algorithm, 2008 International Conference on BioMedical Engineering and Informatics, 978-0-7695-3118-2/08 \$25.00 © 2008 IEEE DOI 10.1109/BMEI.2008.108.
16. Andrzej Krol, Member, IEEE, Ioana L. Coman Member, IEEE, James A. Mandel, Karl Baum, Min Luo, David H. Feiglin, Edward D. Lipson, and Jacques Beaumont Inter-Modality Non-Rigid Breast Image Registration Using Finite-Element Method, 0-7803-8257-9/04/\$20.00 © 2004 IEEE.
17. Francis Arena M.D, Thomas DiCicco, Azad Anand, M.D. , multi-modality data fusion aids early detection of breast cancer Using conventional technology and advanced digital infrared Imaging, Proceedings of the 26th Annual International Conference of the IEEE EMBS San Francisco, CA, USA • September 1-5, 2004, 0-7803-8439-3/04/\$20.00©2004 IEEE.
18. Minavathi, Murali. S, M. S. Dinesh, Detection of Architectural Distortions with Spiculations in Mammograms by analyzing the structure of Showsmammary glands , Proceedings of Fifth Indian International Conference on Artificial Intelligence(IICAI) , Tumkur, Dec-2011, page no: 218-230.
19. Yuji Ikeda, Daisuke Fukuokab, Takeshi Haraa, Hiroshi Fujitaa, Etsuo Takadac, Tokiko Endod, and Takako Moritae, Computerized mass detection in whole breast ultrasound images: Reduction of false positives using bilateral subtraction technique, Medical Imaging 2007, Proc. of SPIE Vol. 6514, 65141T, (2007) · 1605-7422/07.

20. Steve R. Gunn, Support Vector Machines for Classification and Regression, Technical Report, University of Southampton, 1998.
21. Ravishankar Rao and Ramesh C, "Computerized Flow Field Analysis: Oriented Texture Fields", 0162-8828, 1992 IEEE.
22. Minavathi, Murali. S, M. S. Dinesh, Classification of Mass in Breast Ultrasound Images using Image Processing Techniques, International journal of computer applications, march 2012.
23. J. Suckling, D. R. Dance, E. Moskovic, D. J. Lewis, and S. G. Blacker, Segmentation of mammograms using multiple linked self-organizing neural networks, Med. Phys., vol. 22, no. 2, pp. 145–152, Feb. 1995.
24. N. Karssemeyer, Automated classification of parenchymal patterns in mammograms, Phys. Med. Biol., vol. 43, no. 2, pp. 365–378, Feb. 1998.
25. R. J. Ferrari, R. M. Rangayyan, J. E. L. Desautels, and A. F. Frère, Segmentation of mammograms: Identification of the skin boundary, pectoral muscle, and fibroglandular disc, in IWDM 2000: Proc. 5th Int. Workshop Digital Mammography, M. J. Yaffe, Ed., Madison, WI, 2001, pp.
26. F. Georgsson, Algorithms and techniques for computer aided mammographic screening, Ph.D. dissertation, Umeå Univ., Dept. Comput. Sci., Umeå, Sweden, 2001.
27. P. Perona and J. Malik, Scale-space and edge detection using anisotropic diffusion, IEEE Transactions on Pattern Analysis and Machine Intelligence, pp. 629–639, July 1990.
28. M. Mignotte and J. Meunier, "A multiscale optimization approach for the dynamic contour-based boundary detection issue," Comput. Med. Imag. Graph., vol. 25, no. 3, pp. 265–275, May–Jun. 2001.
29. F. Heitz, P. Perez, and P. Bouthemy, "Multiscale minimization of global energy functions in some visual recovery problems," CVGIP: Image Understanding, vol. 59, pp. 125–134, 1994.
30. Tourassi GD, Delong DM, Floyd CE Jr (2006): A study on the computerized fractal analysis of architectural distortion in screening mammograms. Phys Med Biol 1(5),1299-1312.
31. Rangayyan RM, Ayres FJ (2008): Detection of architectural distortion in prior screening mammograms using Gabor filters, phase portraits, fractal dimension, and texture analysis, Int J CARS (2008) 2:347-361.
32. Luan Jiang, MSc, Enmin Song, PhD, Xiangyang Xu, MSc, Guangzhi Ma, MSc, Bin Zheng, PhD: Automated Detection of Breast Mass Spiculation Levels and Evaluation of Scheme Performance1, Academic Radiology, Vol 15, No 12, Dec 2008, 15:1534-1544.
33. Burhenne L J W, Wood S A, D'Orsi C J, Feig S A, Kopans D B, O'Shaughnessy L F, Sickles E A, Tabar L, Vybomy C J and Castellino R A Radiol. 215 554-562.
34. Evans W P, Burhenne L J W, Laurie L, O'Shaughnessy K F and Castellino R A 2002 Radiol. 225 182-189.
35. L. Liberman et al. : The breast imaging reporting and data system: positive predictive value of mammographic features and final assessment categories, AJR. American Journal of Roentgenology. 171 (1), 35 (1998).
36. N. R. Mudigonda, R. M. Rangayyan, and J. E. L. Desautels, "Detection of breast masses in Mammograms by density slicing and texture flow-field analysis", IEEE Trans. Med. Imag., vol. 20, no. 12, pp. 1215–1227, December 2001.
37. Julia E. E. de Oliveira, Thomas M. Deserno and Arnaldo de A. Araujo, "Breast Lesions Classification applied to a reference Database", IEEE and E-MEDISYS 2008 2nd International Conference: E- Medical Systems.
38. Cheng X.-Y., Akiyama L, Itoh K., Wang Y., Taniguchi N. and Nakajima M. (1997) 0-8186- 8183-7/97, IEEE.
39. Horsch K., Giger M. L., Venta L. A. and Vybomy C. J. (2001) Med. Phys., vol. 28, no. 8, pp. 1652–1659.
40. Madabhushi A. and Metaxas D. N. (2003) IEEE Trans. Med. Imag., vol. 22, no. 2, pp. 155–169.
41. Yuji Ikeda, Daisuke Fukuokab, Takeshi Haraa, Hiroshi Fujitaa, Etsuo Takadac, Tokiko Endod, and Takako Moritae (2007) Medical Imaging 2007, Proc. of SPIE Vol. 6514, 65141T.
42. Dar-Ren Chena, T. Ruey-Feng Changb, Chii- Jen Chenb, Ming-Feng Hob, Shou-Jen Kuo, Shou-Tung Chena, Shin-Jer Hungc, Woo Kyung Moon (2005) Journal of Clinical Imaging, 29, 235–245.
43. Yuji Ikeda, Takako Morita, Daisuke Fukuoka, Takeshi Hara, Bert Lee, Hiroshi Fujita, Etsuo Takada, Tokiko Endo (2009) Int J CARS, 4:299–306.